



Integration of a solar heliostat field with humidifier-dehumidifier desalination units to generate electricity and fresh water

Seyyed Masoud Seyyedi^{1,2,*}, Seyyed Mostafa Ghadami^{2,3}

¹Department of Mechanical Engineering, Aliabad Katoul Branch, Islamic Azad University, Aliabad Katoul, Iran

²Energy Research Center, Aliabad Katoul Branch, Islamic Azad University, Aliabad Katoul, Iran

³Department of Electrical Engineering, Aliabad Katoul Branch, Islamic Azad University, Aliabad Katoul, Iran

Article info	Abstract
<p>Keywords: Solar energy Humidifier-dehumidifier Fresh water Electricity cost Cogeneration</p>	<p>One of the most important human needs is fresh water. Production of electricity and fresh water in compliance with environmental issues is a very important issue. In the present work, a solar cogeneration system is proposed for the production of electricity and fresh water. Power system and humidifier-dehumidifier (HDH) units are responsible for electricity and freshwater production, respectively. Firstly, thermodynamic analysis is performed to determine the mass, pressure, temperature and other thermodynamic properties of each flow. An economic analysis is then performed to determine the maximum benefit of the system. The results show that the maximum values for profit and net power are 1164 \$/h and 20468 kW at pressure ratio 6 and 7, respectively. The mass flow rate of fresh water increases 46.4% when mass ratio of water to air goes up from 1.0 to 1.7 at an inlet hot air dry bulb temperature of 83 °C.</p>
<p>Article history: Received: 30 Jun 2024 Accepted: 10 Jul 2024</p>	

1. Introduction

The importance of the environmental pollution indicates that the fossil fuels must be replaced by renewable energy. Solar energy is a renewable source that can be used for a wide range of applications especially for power generation [1]. Fresh water is one

of the most important human needs. Due to the scarcity of fresh water in the world, salt water is usually converted to fresh water by cogeneration systems. Cogeneration systems refer to energy systems that have the ability to produce two useful commodities simultaneously. A good example of cogeneration

* Corresponding author.
E-mail address: s.masoud_seyyedi@aliabadiau.ac.ir (S.M. Seyyedi).

systems are combined heat and power plants, where electricity and useful heat are both produced from one plant. Researchers have proposed many cogeneration or multi-generation systems to produce power, hydrogen, heating, cooling, fresh water etc. Fig.1 represents different methods of water desalination. The standard desalination techniques like multistage flash (MSF), multi-effect (ME), vapor compression (VC) and reverse osmosis (RO) are only reliable for large capacity ranges of 100–50,000 m³/day of fresh water production [2]. These technologies are expensive for small amounts of fresh water, and they cannot be used in locations such as islands and remote areas where there are limited maintenance facilities and energy supply. According to Mistry et al. [3], a fundamental problem with most desalination technologies, including RO, MSF and MED, is that they are very energy intensive.

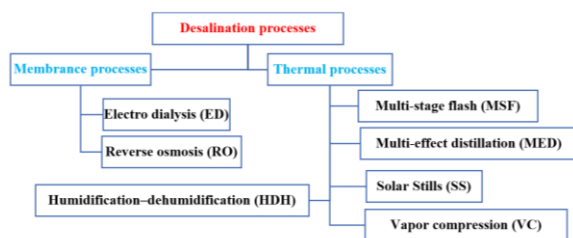


Fig. 1: Different methods of water desalination

Solar desalination can be either direct or indirect [4]. One of the well-known indirect solar desalination systems is the humidification–dehumidification (HDH) distillation process. Solar desalination based on the HDH cycle presents the best method of solar desalination due to overall high-energy efficiency [5]. In 2010, thermodynamic second law analysis was performed for the HDH desalination cycles by Mistry et al. [3]. In 2012, Al-Sulaiman et al. [6] proposed a tri-generation system, based on biomass and analyzed its related efficiencies of energy and exergy. In 2015, Zare [7] evaluated the thermodynamic and economic performance of three arrangements of ORCs in geothermal-based binary power plants; a simple-ORC, which was reported to be the best economically, a regenerative ORC, and an ORC with internal heat exchanger, which was thermodynamically superior. In 2015, the operation of PTSCs in producing freshwater established on HDH desalination system was presented by Sulamian et al. [8]. In the mentioned

system, PTSCs were employed as air heaters. In 2016, Deniz and Çınar [9] explored a freshwater production procedure grounded on HDH and benefitting from solar energy through flat plate solar collectors (FPSCs), from thermodynamic, economic, and environmental viewpoints. The maximum freshly produced water was 1.1 kg/h with an approximate cost rate of 0.1 \$/L. In 2017, Nami et al. [10] proposed a novel cogeneration system, including a gas turbine, a heat recovery steam generator and supercritical recompression CO₂ cycle to produce power and steam. They reported that under the optimized condition the average product unit cost of the system (the cost of produced power and steam) is decreased by 0.56 \$/GJ when compared to the value obtained under a base condition. In 2017, a geothermal based multi-generation energy system, including organic Rankine cycle, domestic water heater, absorption refrigeration cycle and proton exchange membrane electrolyzer, was developed to generate electricity, heating, cooling and hydrogen by Akrami et al. [11]. In 2018, Behnam et al. [12] investigated the effect of different performance parameters on economic and thermodynamic aspects and found that for low geothermal temperatures, the effect of changes in absorber and condenser temperatures is more significant. In 2018, a novel integration of a 1000 MW pressurized water reactor power plant and a gas turbine cycle through a super-heater was proposed by Seyyedi et al. [13]. In 2018, feasibility investigation of a humidification dehumidification (HDH) desalination system driven by an absorption-compression heat pump cycle was carried out by Rostamzadeh et al. [14]. In 2019, Wang et al. [15] devised a novel cogeneration system by combining PV cells with a PEME. They reported an annual H₂ production rate of 47.5 kg per unit area of the PV cell. In 2019, Anvari et al. [16] carried out thermodynamic and environmental assessments for a renewable-based system based on syngas and concentrated solar power (CSP). The combined cycle (a Brayton cycle and a steam Rankine cycle) generates 13.4MW of electricity. In 2020, Ghorbani et al. [17] developed an innovative combined energy system, based on phase change materials (PCM) and an organic Rankine cycle (ORC), to produce power and freshwater. The system was able to produce 3628 kg/h water and 459.9 MW electrical power. In 2020, investigation and economic optimization of a tri-generation system (electricity,

cooling, and freshwater) was accomplished by Gholizadeh et al. [18]. The system was driven by biomass fuel using an HDH unit. In 2021, the simultaneous production of electricity, freshwater, and hydrogen from seawater was proposed by Delpisheh et al. [19]. They concluded that the system's cost per unit exergy increases by increasing current density and reduces by decreasing electrolyzer temperature and desalination top temperature. In 2022, the thermoeconomic analysis of a solar-driven hydrogen production system with proton exchange membrane water electrolysis unit was performed by Seyyedi et al. [20]. In 2020, a good review paper on the HDH techniques was published by Mohamed et al. [21]. According to the studies mentioned above, the combination of Heliostat solar field with HDH system has not been done.

2. System descriptions

Heliostat is a Greek word that means sun, and it is generally referred to a set of mirrors that are located around a rotating axis and are able to continuously reflect sunlight to a specific point or the central receiver. Fig. 2 shows a solar power cycle consisting of an air compressor, a solar heliostat field (to generate hot air) and a gas turbine. Hot air enters the gas turbine to generate power, while the outlet is still at a high temperature.

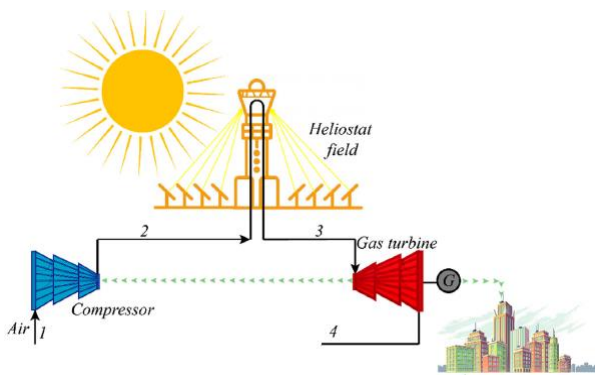


Fig. 2: Schematic of a solar power cycle

Fig.3 represents a desalination system that has a humidification – dehumidification (HDH) distillation process. Hot air enters the humidifier. Then the moist air leaves the humidifier and enters the dehumidifier.

Finally, the cold air leaves the dehumidifier. Distilled water leaves the dehumidifier as a final product.

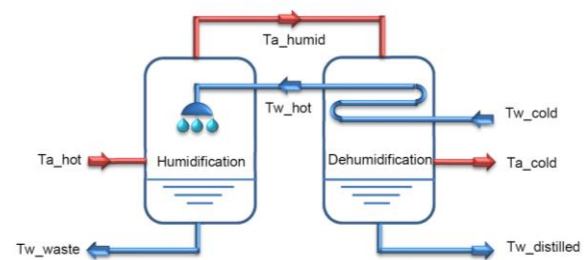


Fig. 3: HDH system

Fig. 4 shows the proposed cogeneration system. In this system, the solar heliostat power cycle is combined with a HDH system by an air heater. The exhaust air from the gas turbine (state 4), which has a high temperature, enters an air heater to heat the air needed (process 6-7) for the desalination system. Sea water enters the dehumidifier (state 9) and brine leaves the humidifier (state 11). Distilled water leaves the dehumidifier as a final product (state 12). Fig. 5 shows the cogeneration system with several desalination units.

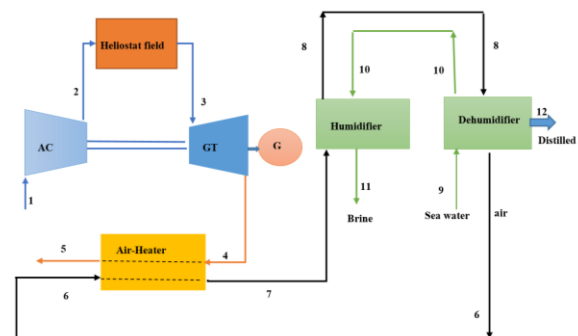


Fig. 4: The proposed solar cogeneration system

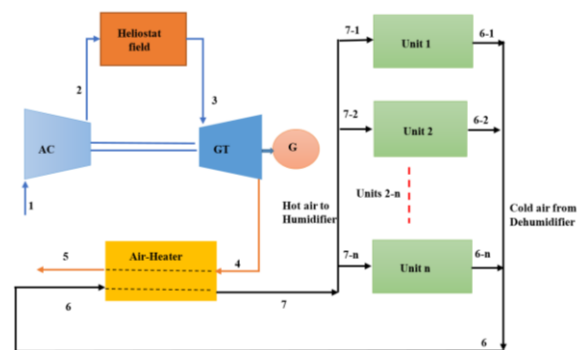


Fig. 5: The Solar cogeneration system with several desalination units

3. Mathematical Modeling

The mass and energy balance equations for each component must be written. Also, an economic model must be developed.

3.1. Thermodynamic analysis

The mass flow rate of each stream is as follows (See Figs. 4 and 5)

$$\dot{m}_1 = \dot{m}_2 = \dot{m}_3 = \dot{m}_4 = \dot{m}_5 = \dot{m}_{\text{air.GT}} \quad (1)$$

$$\dot{m}_6 = \dot{m}_7 = \dot{m}_8 = \dot{m}_{\text{air.HDH}} \quad (2)$$

$$\dot{m}_9 = \dot{m}_{10} = \dot{m}_{\text{water.HDH}} \quad (3)$$

A mass balance on the water vapor in the dehumidifier air stream gives the mass flow rate of product [3]:

$$\dot{m}_p = \dot{m}_{12} = \dot{m}_{\text{air.HDH}}(\omega_8 - \omega_6) \quad (4)$$

Also, a water mass balance in the humidifier shows that:

$$\dot{m}_b = \dot{m}_{11} = \dot{m}_{\text{water.HDH}} - \dot{m}_p \quad (5)$$

It should be mentioned that \dot{m}_p is the mass flow rate of distilled water (for a single unit) whereas the mass flow rate of fresh water (for several units) can be calculated by:

$$\dot{m}_{\text{FW}} = N_{\text{HDH}} \times \dot{m}_p \quad (6)$$

The mass ratio (MR) of water to air is introduced as follows [3]:

$$MR = \frac{\dot{m}_{\text{water.HDH}}}{\dot{m}_{\text{air.HDH}}} \quad (7)$$

➤ *Air compressor (AC):*

The outlet temperature of air compressor can be calculated by [13]:

$$T_2 = T_1 \left[1 + \frac{1}{\eta_{\text{AC}}} \left(\left(\frac{P_2}{P_1} \right)^{\frac{k-1}{k}} - 1 \right) \right] \quad (8)$$

The air compressor work is calculated as follows:

$$\dot{W}_{\text{AC}} = \dot{m}_1 c_{p,\text{air}} (T_2 - T_1) \quad (9)$$

➤ *Solar Heliostat field (SHF):*

The total amount of solar energy in heliostats is given by Eqs. (10) and (11) [22].

$$\dot{Q}_{\text{sun}} = A_{\text{hel}} \times N_{\text{hel}} \times DNI \quad (10)$$

$$\dot{Q}_h = \eta_{\text{hel}} \times \dot{Q}_{\text{sun}} \quad (11)$$

Heat losses can be quantified by Eq. (12).

$$\dot{Q}_{\text{loss}} = h_{\text{air}} A_h (T_r - T_0) + \sigma \varepsilon A_h (T_r^4 - T_0^4) \quad (12)$$

$$h_{\text{air}} = 10.45 - v_{\text{air}} + 10\sqrt{v_{\text{air}}} \quad (13)$$

Finally, the heat transfer rate between air and receiver can be calculated by:

$$\dot{Q}_r = \dot{Q}_h - \dot{Q}_{\text{loss}} = \dot{m}_2 (h_3 - h_2) \quad (14)$$

➤ *Gas turbine (GT):*

The outlet temperature of gas turbine can be calculated by[13]:

$$T_4 = T_3 \left[1 - \frac{1}{\eta_{\text{GT}}} \left(1 - \left(\frac{P_3}{P_4} \right)^{\frac{1-k}{k}} \right) \right] \quad (15)$$

The gas turbine work is calculated as follows:

$$\dot{W}_{\text{GT}} = \dot{m}_3 c_{p,\text{air}} (T_3 - T_4) \quad (16)$$

The net work of solar power cycle is calculated as follows:

$$\dot{W}_{\text{net}} = \dot{W}_{\text{GT}} - \dot{W}_{\text{AC}} \quad (17)$$

➤ *Air Heater (AH):*

The energy balance for air heater can be written as follows:

$$\dot{m}_4 c_p (T_4 - T_5) = \dot{m}_6 (h_7 - h_6) \quad (18)$$

➤ *HDH system:*

The energy balance for humidifier and dehumidifier can be written respectively as follows (for a single desalination unit according to Fig. 4):

a. Humidifier

$$\dot{m}_7 (h_7 - h_8) = \dot{m}_{11} h_{11} - \dot{m}_{10} h_{10} \quad (19)$$

b. Dehumidifier

$$\dot{m}_8 (h_8 - h_6) - \dot{m}_{12} h_{12} = \dot{m}_9 (h_{10} - h_9) \quad (20)$$

Also, the efficiency of humidifier (ε_H) and dehumidifier (ε_D) can be calculated respectively [3]:

$$\varepsilon_{\text{H,air}} = (h_7 - h_8) / (h_7 - h_{8,s}) \quad (21)$$

where $h_{8,s}$ is maximum enthalpy of humid air from humidifier.

$$\varepsilon_{\text{H,water}} = (h_{11} - h_{10}) / (h_{11,s} - h_{10}) \quad (22)$$

where $h_{11,s}$ is maximum enthalpy of waste water from humidifier.

$$\varepsilon_H = \max(\varepsilon_{\text{H,air}} \text{ and } \varepsilon_{\text{H,water}}) \quad (23)$$

$$\varepsilon_{D,air} = (h_8 - h_6)/(h_8 - h_{6,s}) \quad (24)$$

where $h_{6,s}$ is maximum enthalpy of cold air from dehumidifier.

$$\varepsilon_{D,water} = (h_{10} - h_9)/(h_{10,s} - h_9) \quad (25)$$

where $h_{10,s}$ is maximum enthalpy of outlet water from dehumidifier.

$$\varepsilon_D = \max(\varepsilon_{D,air} \text{ and } \varepsilon_{D,water}) \quad (26)$$

3.2. Performance parameters

The gained output ratio (GOR) is a non-dimensional measure of the amount of product produced for a given heat input. Here, it is defined as [9]:

$$GOR = \frac{\dot{m}_p h_{fg}}{\dot{Q}_{in}} \quad (27)$$

where h_{fg} is the heat of vaporization at the dead state (ambient conditions). The input heat rate to HDH system can be calculated as follows:

$$\dot{Q}_{in} = \dot{m}_6(h_7 - h_6) \quad (28)$$

The efficiency of cogeneration system can be evaluated as follows:

$$\eta_{th} = \frac{\dot{W}_{net} + \dot{m}_{FW} h_{fg}}{\dot{Q}_h} \quad (29)$$

For more details see Refs. [3, 9, 13].

3.3. Thermo-economic analysis

In this section, the thermo-economic model is presented. The cost rate of each component (\dot{Z}_k) is given by [20]:

$$\dot{Z}_k = \frac{\varphi \times CRF \times PW}{\tau} \quad (30)$$

where the capital recovery factor (CRF) is a function of interest rate (i) and the lifetime of components (n) and can be calculated by:

$$CRF = \frac{i \times (i + 1)^n}{(i + 1)^n - 1} \quad (31)$$

Also, the operation time of the system and the coefficient operation are considered 12 hours per day (from 6 to 18) and 0.85, respectively. Therefore, $\tau = 0.85 \times 12 \times 365 = 3723$ hr.

The present worth is defined as:

$$PW = TCI - SV(PWF) \quad (32)$$

where

$$PWF = \frac{1}{(i + 1)^n} \quad (33)$$

and

$$SV = \mu (TCI) \quad (34)$$

where μ is the salvage percentage. Appendix A presents the total capital investment (TCI) cost for each component.

The average cost of electricity (c_W in \$/kWh) is obtained by:

$$c_W = (\dot{Z}_{AC} + \dot{Z}_{SHF} + \dot{Z}_{GT})/\dot{W}_{net} \quad (35)$$

The average cost of fresh water (c_{FW} in \$/m³) is obtained by:

$$c_{FW} = \frac{[\dot{Z}_{AH} + (\dot{Z}_H + \dot{Z}_D) \times N_{HDH}]}{(\dot{m}_{FW} \times 3600/1000)} \quad (36)$$

Revenue (\dot{R}) means money that can be earned from the sale of electricity and fresh water and can be calculated as follows:

$$\dot{R} = C_{sale.W} \times \dot{W}_{net} + C_{sale.FW} \times \dot{m}_{FW} \quad (37)$$

where $C_{sale.W} = 0.121$ \$/kwh [20] and $C_{sale.FW} = 100$ \$/m³ [21]:

Finally, Profit can be obtained by:

$$\text{Profit} = \dot{R} - (\dot{Z}_{total} + \dot{Z}_{land}) \quad (38)$$

where

$$\dot{Z}_{total} = \dot{Z}_{AC} + \dot{Z}_{SHF} + \dot{Z}_{GT} + \dot{Z}_{AH} + (\dot{Z}_H + \dot{Z}_D) \times N_{HDH} \quad (39)$$

and

$$\dot{Z}_{land} = 0.1 \times \dot{Z}_{total} \quad (40)$$

4. Results and discussion

Here, the effects of the main parameters on the performance of the system are investigated. Modeling of the system was performed in EES software. Table 1 presents the predefined values for modeling the problem. Also, Table 2 presents the results based on the values of Table 1. Table 3 shows the effects of variation of inlet hot air dry bulb temperature (T_7) on the main results of the system. The results show that the profit increases 1105 \$/h to 1218 \$/h (10.2% increasing) when T_7 increases from 65 °C to 75 °C.

Table 1: Modeling input parameters [3, 13, 22]

Parameter	Definition	Amount
Power system		
T_0	Ambient temperature	20 °C
P_0	Ambient pressure	101.3 kPa
DNI	Direct normal irradiance	850 W/m ²
N_{hel}	Number of heliostats	1500
A_r	The area of heliostats	60 m ²
T_r	The receiver local temperature	1000 °C
T_3	The gas turbine inlet temperature	750 °C
η_{hel}	Heliostat efficiency	0.71
ϵ_r	Surface emissivity of the receiver	0.88
v_w	Wind speed	5 m/s
r_p	Compressor pressure ratio	6
η_{GT}	Gas turbine efficiency	0.85
η_{AC}	Air compressor efficiency	0.82
HDH system		
\dot{m}_{air}	Air mass flow rate in HDH system	5 kg/s
MR	Mass ratio of water to air	1.2
$T_{w.in} = T_9$	Inlet cold water temperature	20 °C
$T_{hot.air} = T_7$	inlet hot air dry bulb temperature	70 °C
$\phi_{hot.air} = \phi_7$	Inlet hot air relative humidity	40 %
ϵ_H	Humidifier Efficiency	0.85
ϵ_D	Dehumidifiers Efficiency	0.95
N_{HDH}	Number of HDH units	10
Economic parameters		
τ	Working hour per year	3723 hr
i	Interest rate	0.12
n	Lifetime of components	25 year
ϕ	Maintenance factor	1.06
μ	Salvage percentage	15 %
$c_{sale.elec}$	Selling price of electricity	0.12 \$/kWh
$c_{sale.FW}$	Selling price of fresh water	100 \$/m ³

Tables 2: Results based on the values of Table 1

Parameter	Value
$\eta_{th.t}$	0.2324
GOR	0.5079
T_5 (K)	618.1
\dot{Z}_T (\$/h)	1865
$c_{cost.elec}$ (\$/kWh)	0.06218
$c_{cost.FW}$ (\$/m ³)	78.75
\dot{W}_{net} (kW)	20160
\dot{m}_{FW} (kg/s) ^a	2.158
Profit (\$/h)	1164

$$^a \dot{m}_{FW} = 2.158 \frac{\text{kg}}{\text{s}} = 7768.8 \frac{\text{kg}}{\text{h}} = 186.45 \frac{\text{m}^3}{\text{day}}$$

Fig. 6 shows the net power and profit versus the pressure ratio. The values of both curves firstly increase, reach to a maximum value and then decrease when the pressure ratio goes up. Therefore, there is a maximum value for profit and net power at pressure ratio 6 and 7, respectively. These values are 1164 \$/h and 20468 kW.

Table 3: The effects of T_7 on the main results

	$T_7 = 65$ °C	$T_7 = 70$ °C	$T_7 = 75$ °C
GOR	0.524	0.5079	0.4864
$\eta_{th.t}$	0.2246	0.2324	0.2407
\dot{m}_{FW} (kg/s)	1.809	2.158	2.528
\dot{Z}_T (\$/h)	1805	1865	1938
$c_{cost.FW}$ (\$/m ³)	84.73	78.75	75.17
Profit (\$/h)	1105	1164	1218

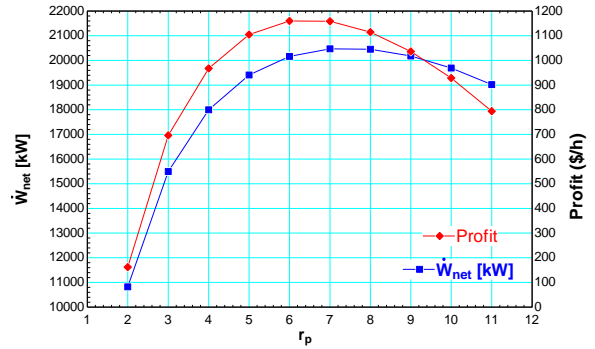


Fig. 6: Variations of \dot{W}_{net} and profit versus r_p

Fig. 7 presents the profit versus the pressure ratio at different values of gas turbine inlet temperature (T_3). The maximum values of profit occur at pressure ratio 6, 7 and 8 for gas turbine inlet temperature 750°C, 800°C and 850°C, respectively. These values are 1164 \$/h, 1328 \$/h and 1478 \$/h, respectively. The figure shows that profit increases when the gas turbine inlet temperature increases. For example, profit increases from 1164 \$/h to 1410 \$/h (21.1% increasing) when the gas turbine inlet temperature goes up from 750°C to 850°C at $r_p = 6$.

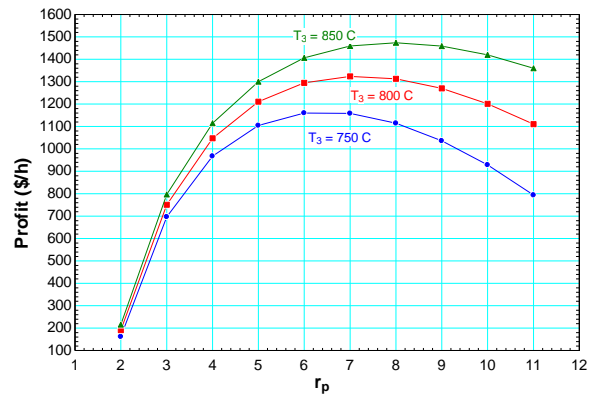


Fig. 7: Variations of profit versus r_p at different values of T_3

Figs. 8 and 9 show the effects of gas turbine efficiency and air compressor efficiency on the profit at different

values of pressure ratio, respectively. The figures show that the values of profit increase with increasing the values of gas turbine efficiency or air compressor efficiency for each value of pressure ratio. For example, profit increases from 917 \$/h to 1371 \$/h (49.5% increasing) when the gas turbine efficiency ascends from 0.82 to 0.88 at $r_p = 6$. Also, profit increases from 1072 \$/h to 1239 \$/h (15.6% increasing) when the air compressor efficiency ascends from 0.80 to 0.84 at $r_p = 6$.

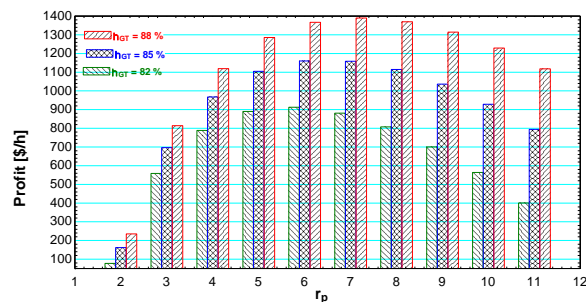


Fig. 8: Variations of profit versus r_p at different values of η_{GT}

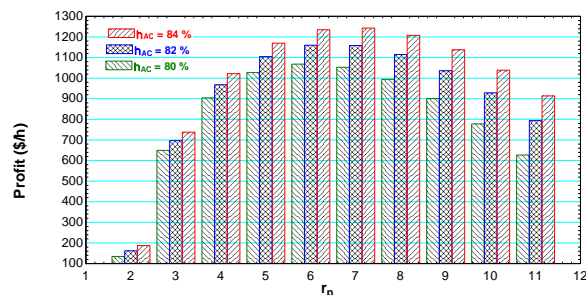


Fig. 9: Variations of profit versus r_p at different values of η_{AC}

Fig. 10 demonstrates the profit versus the mass ratio of water to air (MR) at different values inlet hot air dry bulb temperature (T_7). The values of profit firstly increase, reach to a maximum value and then decrease when versus the mass ratio of water to air goes up. The maximum values of profit are 1515 \$/h, 1649 \$/h and 1728 \$/h for $T_7 = 80^\circ\text{C}$, $T_7 = 82^\circ\text{C}$ and $T_7 = 83^\circ\text{C}$, that occur at $MR = 1.3$, $MR = 1.5$ and $MR = 1.6$, respectively. These values indicate that the optimum value of mass ratio of water to air must be determined for each value of inlet hot air dry bulb temperature.

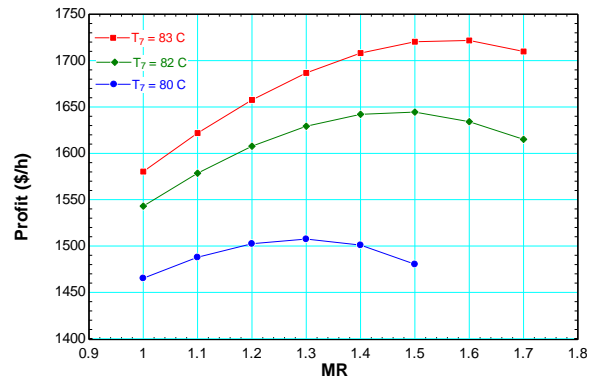


Fig. 10: Variations of profit versus MR at different values of T_7

Fig. 11 illustrates the mass flow rate of fresh water for different values of MR at $T_7 = 82^\circ\text{C}$ and $T_7 = 83^\circ\text{C}$. As it can be seen, the mass flow rate of fresh water increases with increasing the values of MR for each value of T_7 . For example, \dot{m}_{FW} increases from 3.044 kg/s to 4.455 kg/s (46.4% increasing) when MR ascends from 1.0 to 1.7 at $T_7 = 83^\circ\text{C}$.

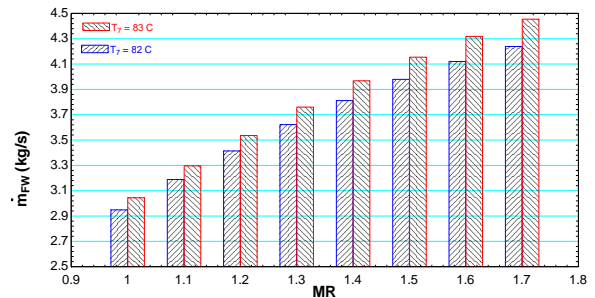


Fig. 11: Variations of \dot{m}_{FW} versus MR at different values of T_7

Figs. 12 and 13 show the GOR, profit, the mass flow rate of fresh water and cost of fresh water versus the inlet hot air dry bulb temperature (T_7) at two different values of the inlet hot air relative humidity (ϕ_7). As it can be seen, the profit, GOR at $\phi_7 = 0.5$ and the mass flow rate of fresh water increase when T_7 increases whereas the cost of fresh water decreases with increasing the T_7 . There is a minimum value for GOR at $\phi_7 = 0.4$ when $T_7 = 74^\circ\text{C}$. For example, profit increases from 1398 \$/h to 1912 \$/h (36.8 % increasing) and GOR increases from 0.5534 to 0.6450 (16.5 % increasing) when T_7 ascends from 70°C to 80°C at $\phi_7 = 0.5$. Also, \dot{m}_{FW} increases from 2.698 kg/s to 3.921 kg/s (45.3 % increasing) while c_{FW} decreases from 59.27 \$/m³ to 36.08 \$/m³ (39.1 % decreasing) when T_7 ascends from 70°C to 80°C at $\phi_7 = 0.5$.

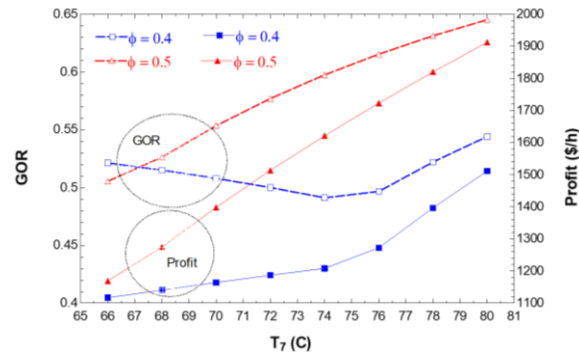


Fig. 12: Variations of GOR and Profit versus T_7 at two values of ϕ_7

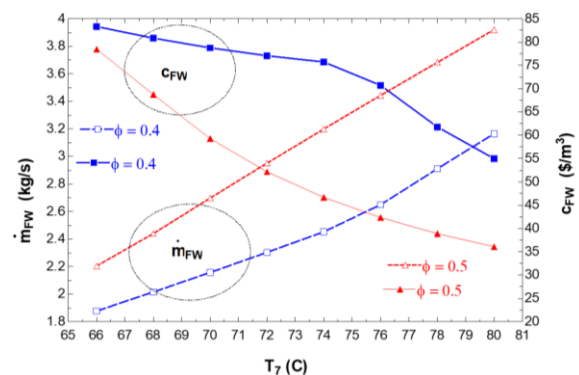


Fig. 13: Variations of \dot{m}_{FW} and c_{FW} versus T_7 at two values of ϕ_7

Fig. 14 shows the variations of profit versus the lifetime of the system (n), at three different values of interest rate (i). Profit increases when the values of lifetime ascend for each value of interest rate. Also, profit ascends with descending the interest rate for a constant value of a lifetime. For example, the value of profit increases from 786.3 \$/h to 893.9 \$/h (13.7% increasing) when n increases from 20 to 29 years for $i = 14\%$.

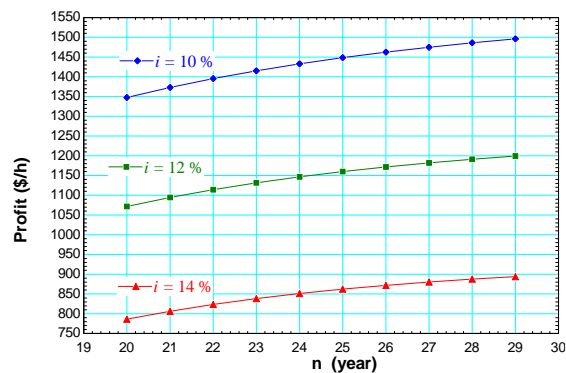


Fig. 14: Variations profit versus the lifetime of the system (n) at three different values of interest rate (i)

5. Conclusion

In the present work, a solar cogeneration system analyzed thermodynamically and economically. The power system and humidifier-dehumidifier (HDH) units are responsible for electricity and freshwater production, respectively. Modeling of the system was performed in EES software where the effects of important parameters were investigated on the amount of fresh water, the net produced power, and net profit of the products. The main results can be summarized as follow:

- (a) The maximum value of profit and net power are 1164 \$/h and 20468 kW that occur at pressure ratio 6 and 7, respectively.
- (b) The profit increases 10.2% when T_7 increases from 65 °C to 75 °C.
- (c) The profit increases 21.1% when the gas T_3 goes up from 750°C to 850°C at $r_p = 6$.
- (d) The profit increases 49.5% when the η_{GT} ascends from 0.82 to 0.88 at $r_p = 6$.
- (e) The profit increases 15.6% when the η_{AC} ascends from 0.80 to 0.84 at $r_p = 6$.
- (f) The \dot{m}_{FW} increases 46.4% when MR ascends from 1.0 to 1.7 at $T_7 = 83$ °C.
- (g) The profit increases 36.8 % and GOR increases 16.5 % when T_7 ascends from 70 °C to 80 °C at $\phi_7 = 0.5$.
- (h) The \dot{m}_{FW} increases 45.3 % while c_{FW} decreases 39.1% when T_7 ascends from 70 °C to 80 °C at $\phi_7 = 0.5$.
- (i) The value of profit 13.7% when n increases from 20 to 29 years for $i = 14\%$.

References

[1] SM. Seyyedi, “thermoeconomic analysis of a steam rankine cycle integrated with parabolic trough solar collectors” Journal of Applied Dynamic Systems and Control, Vol.4, No.1, (2021), 1- 7.

[2] H.E.S. Fath, “Desalination technology, The role of Egypt in region IWT C” Alexandria, Egypt, (2000).

[3] Karan H. Mistry, John H. Lienhard V, Syed M. Zubair, “Effect of entropy generation on the performance of humidification-dehumidification desalination cycles” international Journal of Thermal Sciences 49 (2010), 1837-1847.

- [4] H. Fath, "Solar desalination promising alternative for fresh water production with free energy simple technology and clean environmental", *Desalination*, 116 (1998) 45–56.
- [5] Sandeep Parekh, M. M. Farid, J. R. Selman, A. I. Hallaj, "Solar desalination with a humidification-dehumidification technique - a comprehensive technical review", *Desalination* 160 (2004) 167-186.
- [6] Al-Sulaiman FA, Dincer I, Hamdullahpur F. "Energy and exergy analyses of a biomass trigeneration system using an organic Rankine cycle". *Energy* 45(1), (2012); 975-85
- [7] V. Zare, "A comparative exergoeconomic analysis of different ORC configurations for binary geothermal power plants", *Energy Convers Manage.* 105 (2015) 127–138.
- [8] FA. Al-Sulaiman, MI. Zubair, M. Atif, P. Gandhidasan, SA. Al-Dini, MA. Antar, "Humidification dehumidification desalination system using parabolic trough solar air collector. *Appl Therm Eng* 75 (2015) 809–16.
- [9] E. Deniz, S. Çınar, "Energy, exergy, economic and environmental (4E) analysis of a solar desalination system with humidification-dehumidification", *Energy Convers Manage* 126 (2016);12–9.
- [10] H. Nami, SMS. Mahmoudi, A. Nemati, "Exergy, economic and environmental impact assessment and optimization of a novel cogeneration system including a gas turbine, a supercritical CO₂ and an organic Rankine cycle (GT-HRSG/SCO₂)" *Appl Therm Eng* 110, (2017) 1315-30.
- [11] E. Akrami, A. Chitsaz, H. Nami, S.M.S. Mahmoudi, "Energetic and exergoeconomic assessment of a multi-generation energy system based on indirect use of geothermal energy", *Energy* 124 (2017) 625-639.
- [12] P. Behnam, A. Arefi, M. B. Shafii, "Exergetic and thermoeconomic analysis of a trigeneration system producing electricity, hot water, and fresh water driven by low-temperature geothermal sources", *Energy Convers Manage.* 157 (2018) 266–276.
- [13] S.M. Seyyedi, M. Hashemi-Tilehnoee, M.A. Rosen, "Exergy and exergoeconomic analyses of a novel integration of a 1000 MW pressurized water reactor power plant and a gas turbine cycle through a superheater", *Annals of Nuclear Energy* 115 (2018) 161–172.
- [14] H. Rostamzadeh, A. Shekari Namin, H. Ghaebi, M. Amidpour, "Performance assessment and optimization of a humidification dehumidification (HDH) system driven by absorption-compression heat pump cycle", *Desalination* 447 (2018) 84–101.
- [15] H. Wang, W. Li, T. Liu, X. Liu, X. Hu, "Thermodynamic analysis and optimization of photovoltaic/thermal hybrid hydrogen generation system based on complementary combination of photovoltaic cells and proton exchange membrane electrolyzer", *Energy Convers Manage.* 183 (2019) 97–108.
- [16] S. Anvari, S. Khalilarya, V. Zare, "Power generation enhancement in a biomass based combined cycle using solar energy: thermodynamic and environmental analysis", *Appl Therm Eng* 153 (2019) 128-141.
- [17] B. Ghorbani, R. Shirmohammadi, M. Mehrpooya, "Development of an innovative cogeneration system for fresh water and power production by renewable energy using thermal energy storage system", *Sustain Energy Technol Assessments* 37 (2020) 100572.
- [18] T. Gholizadeh, M. Vajdi, H. Rostamzadeh. "Exergoeconomic optimization of a new trigeneration system driven by biogas for power, cooling, and freshwater production", *Energy Convers Manage* 205 (2020) 112417.
- [19] M. Delpisheh, M. Abdollahi M. Haghghi, M. Mehrpooya, A. Chitsaz, H. Athari, "Design and financial parametric assessment and optimization of a novel solar-driven freshwater and hydrogen cogeneration system with thermal energy storage", *Sustainable Energy Technologies and Assessments* 45 (2021) 101096.
- [20] S.M. Seyyedi, M. Hashemi-Tilehnoee, M. Sharifpur, "Thermoeconomic analysis of a solar-driven hydrogen production system with proton exchange membrane water electrolysis unit", *Thermal Science and Engineering Progress*, 30 (2022) 101274.
- [21] A. S. A. Mohamed, M. Salem Ahmed, M. Maghrabee, A. G. Shahdy, "Desalination process using humidification–dehumidification technique: A detailed review", *Int J Energy Res.* 2020;1–52.
- [22] E. Assareh, M. Delpisheh, S. M. Alirahmi, S. Tafi, M. Carvalho, "Thermodynamic-economic optimization of a solar-powered combined energy system with desalination for electricity and freshwater production" *Smart Energy* 5 (2022) 100062.

Appendix A

The total capital investment (TCI) cost for each component is represented in Table A.

Table A: Economic cost equations for the components [19,20, 22]

Component	Purchase cost equation
Air Compressor (AC)	$TCI_{AC} = 75 \times \dot{m}_1 \left(\frac{1}{0.9 - \eta_{AC}} \right) \left(\frac{P_2}{P_1} \right) \ln \left(\frac{P_2}{P_1} \right)$
Gas Turbine (GT)	$TCI_{GT} = 479.3 \times \dot{m}_3 \left(\frac{1}{0.92 - \eta_{GT}} \right) \ln \left(\frac{P_3}{P_4} \right) [1 + \exp(0.036 \times T_3 - 54.4)]$
Solar Heliostat Field (SHF)	$TCI_{hel} = 150 \times A_{hel} \times N_{hel}$ $TCI_{rec} = A_{rec} \times (79 \times T_{rec} - 42000)$
Air Heater (AH)	$TCI_{AH} = 2290 \left(\frac{\dot{m}_4 (h_4 - h_5)}{U_{AH} \times \Delta T_{LMTD}} \right)$ where $U_{AH} = 0.018 \text{ kW}/(\text{m}^2\text{K})$ $\Delta T_{LMTD,AH} = \frac{(T_4 - T_7) - (T_5 - T_6)}{\ln[(T_4 - T_7)/(T_5 - T_6)]}$
Humidifiers (H)	$TCI_H = 746.749 \times (\dot{m}_{10})^{0.79} \times R_{1,H}^{0.57} \times R_{2,H}^{-0.9924} \times (0.022 \times T_{wb,8} + 0.39)^{2.447}$ where $R_{1,H} = T_{10} - T_{11}$ and $R_{2,H} = T_8 - T_{wb,8}$
Dehumidifiers (D)	$TCI_D = 2143 (A_D)^{0.514}$ where $U_D = 1.4 \text{ kW}/(\text{m}^2\text{K})$ $\Delta T_{LMTD,D} = \frac{(T_8 - T_{10}) - (T_6 - T_9)}{\ln[(T_8 - T_{10})/(T_6 - T_9)]}$ and $A_D = Q_D / (U_D \times \Delta T_{LMTD,D})$

It should be mentioned that for updating the TCI values to the original year, Eq. (A) can be used:

$$\text{Original cost} = \text{cost at reference year} \times \frac{\text{cost index for the original year}}{\text{cost index for the reference year}} \quad (\text{A})$$